

Threshold control in VCSELs by proton implanted depth*

ZHAO Hong-dong (赵红东)^{1**}, SUN Mei (孙梅)¹, WANG Wei (王伟)¹, MA Lian-xi (马连喜)², LIU Hui-li (刘会丽)¹, LI Wen-chao (李文超)¹, and LIU Qi (刘琦)¹

1. College of Information Engineering, Hebei University of Technology, Tianjin 300401, China

2. Department of Physics, Blinn College, TX 77805, USA

(Received 11 April 2011)

©Tianjin University of Technology and Springer-Verlag Berlin Heidelberg 2011

The proton implantation is one of key procedures to confine the current diffusion in vertical cavity surface emitting lasers (VCSELs), in which the proton implanted depth and profile are main parameters. Threshold characteristics of VCSELs with various proton implanted depths are studied after optical, electrical and thermal fields have been simulated self-consistently in three dimensions. It is found that for VCSELs with confinement radius of 2 μm , increasing proton implanted depth can reduce the injected current threshold power and enhance the laser temperature in active region. Numerical results also indicate that there are optimal values for current aperture in proton implanted VCSELs. The minimum injected current threshold can be achieved in VCSELs with proton implantation near the active region and confinement radius of 1.5 μm , while the VCSELs with proton implantation in the middle of p-type distributed Bragg reflectors (DBRs) and confinement radius of 2.5 μm can realize the minimum temperature.

Document code: A **Article ID:** 1673-1905(2011)04-0263-3

DOI 10.1007/s11801-011-9246-4

VCSELs are widely used for optical communications and interconnections because of the greatly improved far-field divergence angle^[1-4]. Proton implantation and selective oxide have been used to confine the laser threshold current^[5,6]. The proton implanted depth and profile are two main parameters to affect the threshold current in VCSELs. A high power VCSEL with the maximum continuous wave optical output of 46 mW at room temperature was reported^[7], and various studies on thermal fields were presented in Refs.[8-13]. However, the influence of proton implanted depth on threshold thermal fields and other characteristics of VCSELs were not given in these studies.

The purpose of this work is to find the optimal threshold current in VCSELs for different implanted depths.

The laser is sandwiched between a pair of p and n type DBRs consisting of 20 and 27 alternating quarter-wavelength layers of AlAs and $\text{Al}_{0.16}\text{Ga}_{0.84}\text{As}$, respectively. The active region is made up of three undoped $\text{In}_{0.2}\text{Ga}_{0.8}\text{As}$ quantum wells (QWs) separated by the 100 \AA GaAs layer. The thickness of QW is 80 \AA . In our simulation, the device is fabricated by using the H^+ implantation for lateral current confinement, and the potential satisfies Poisson's equation in substrate, p type and n type DBRs.

$$\frac{\partial^2 V(r, z)}{\partial r^2} + \frac{1}{r} \frac{\partial V(r, z)}{\partial r} + \frac{\partial^2 V(r, z)}{\partial z^2} = \rho . \quad (1)$$

The injected current density is

$$\mathbf{J}(r, z) = -\sigma \nabla V(r, z) , \quad (2)$$

where σ is conductivity. The carrier density N diffusion in the active region can be written as

$$D_n \nabla^2 N(r) - BN^2(r) - \frac{N(r)}{\tau_s} - \frac{g(N(r))P_a |\bar{E}_i|^2}{h\nu} + \frac{J}{ed} = 0, \quad (3)$$

where d is the thickness of active region, and D_n is the diffusion constant. The optical transverse i -mode $\psi_i(r)$ in VCSELs is governed by

$$\frac{1}{r} \frac{\partial}{\partial r} \left(r \frac{\partial \psi_i(r)}{\partial r} \right) + \left(k_0^2 \frac{\epsilon}{\epsilon_0} - \frac{m^2}{r^2} - \beta_{zi}^2 \right) \psi_i(r) = 0 . \quad (4)$$

The steady-state thermal conduction equation in the laser is written as

$$\frac{1}{r} \frac{\partial}{\partial r} \left(r \frac{\partial T(r, z)}{\partial r} \right) + \frac{\partial^2 T(r, z)}{\partial z^2} + \frac{1}{\kappa_i} Q_i(r, z) = 0 . \quad (5)$$

* This work has been supported by the Natural Science Foundation of Hebei Province (No.F2007000096), and the Research Foundation for the Doctoral Program of Higher Education of China (No.20070080001).

** E-mail: zhaohd3000@sina.com.cn

The resistivities in p type DBR, n type DBR and substrate are $2.3 \times 10^{-3} \Omega \cdot m$, $3.19 \times 10^{-4} \Omega \cdot m$ and $4 \times 10^{-5} \Omega \cdot m$, respectively. Other parameters of the investigated VCSELs, such as energy gaps, thermal conductivities, absorption coefficients, refractivity etc., can be found in Refs.[8-13]. Fig.1 shows the threshold potentials of two VCSELs with the same proton implanted aperture radius ($S=2 \mu m$), but the implanted depths are near the active region and in the middle of p type DBR, respectively. Here H_p represents the thickness of p type DBR and L is the distance from the location of proton implantation to the active region. The step current is formed in the VCSEL with proton implantation near the active region, while the proton implantation in the middle of p type DBR ($L=H_p/3$) leads to gradually changing current, as shown in Fig.2(a). Such phenomena are related with that the proton implantation confines the carries to diffuse, and the current cannot spread before it comes into active region.

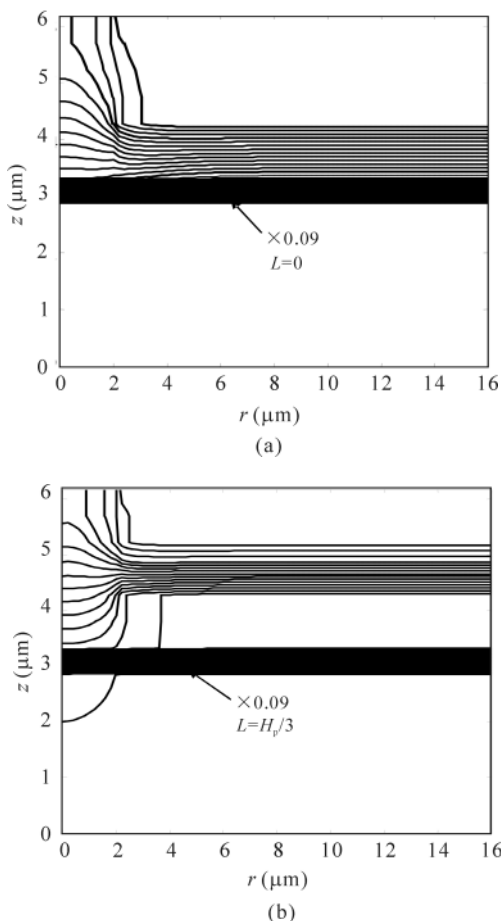
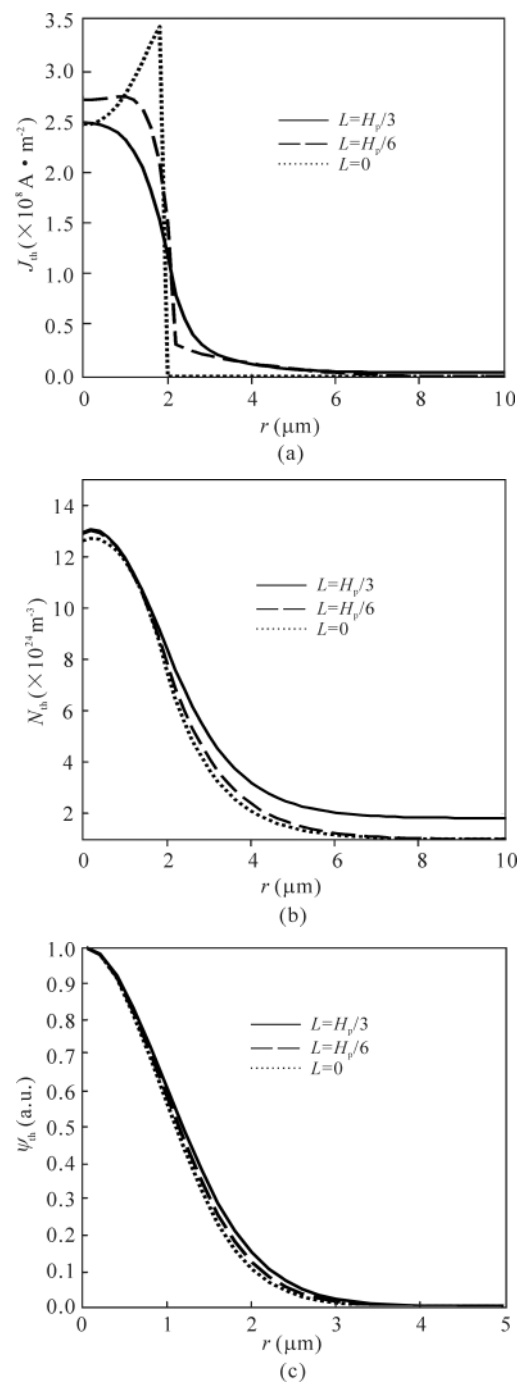


Fig.1 Threshold potentials in VCSELs with $S=2 \mu m$ and the proton implantation (a) near the active region and (b) in the middle of p type DBR

Fig.2(b), (c) and (d) show the distributions of carrier, optical field and temperature in VCSELs with different proton implanted depths. The distributions of carrier and optical

field exhibit a tendency of becoming narrow when proton implanted depths are increased. On the other hand, the laser will be balanced as the heat diffuses into the heat sink and air by heat transmission. Because the main of current is transmitted in the active region for increasing the proton implanted depth, relatively high temperature is observed in the VCSEL with $L=0$.

The injected current threshold power and maximum temperatures versus aperture radius S are given in VCSELs with proton implantation near the active region (Figs.3 and 4). It is found that the current threshold power is dropped and the



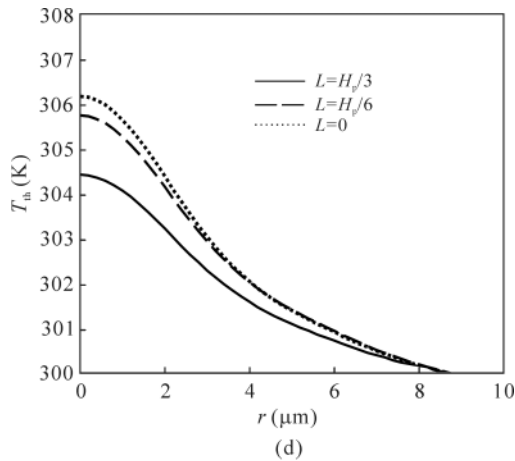


Fig.2 Threshold characteristics of the proton implanted VCSELs: (a) Injected current density; (b) Carrier density; (c) Fundamental mode; (d) Temperature

temperature is improved with decreasing the proton implanted depth. On the other hand, there are optimal current apertures in proton implanted VCSELs. The threshold current cannot be infinitely reduced by decreasing aperture radius, because

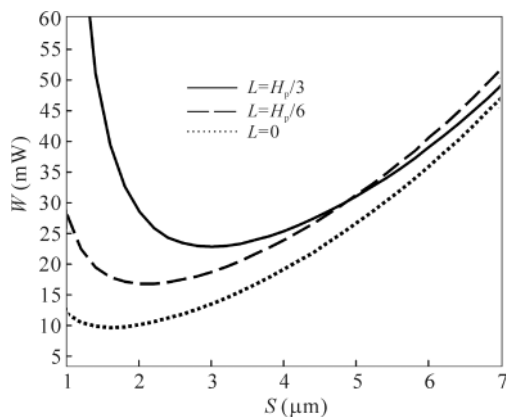


Fig.3 Injected current threshold power values for different implanted depths in VCSELs

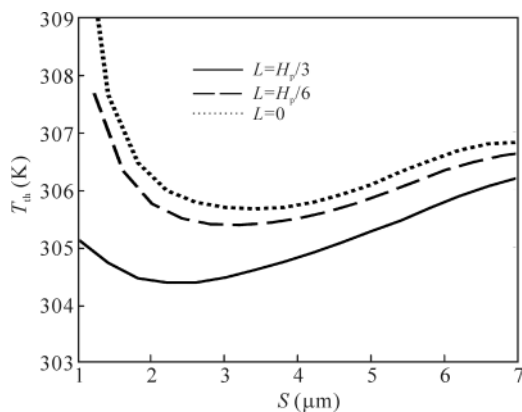


Fig.4 Maximum temperatures for different implanted depths in VCSELs

too small current aperture also damages the injected current threshold power. The lowest injected current power can be achieved in the VCSEL with confinement radius of 1.5 μm and proton implantation near the active region. The lowest temperature is found in the VCSEL with confinement radius of 2.5 μm and proton implantation in the middle of DBR.

The injected current threshold power depends on the size and position of the injected current aperture. We have presented a numerical model for the simulation of VCSELs with different proton implanted depths. The current, carrier and temperature profiles are simulated self-consistently. The injected current distribution can be controlled by proton implanted depth, which is different from the Gaussian function. When the proton implanted position is near the active region, the injected current threshold power is reduced and the temperature is improved due to the step injected current in VCSELs. The performance of VCSELs can be improved with proton implantation near the active region, and the laser threshold would be damaged if proton implantation comes into the active region. The lowest injected current power in the VCSEL can be realized by using confinement radius in scope of 1.5 μm–3 μm. The lowest temperature is obtained in the VCSEL with confinement radius from 2 μm to 4 μm.

References

- [1] M. Ortsiefer, M. Görblich, Y. Xu, E. Rönneberg, J. Rosskopf, R. Shau and M. C. Amann, *IEEE Photonics Technology Letters* **22**, 15 (2010).
- [2] HU Yong-sheng, YE Shu-juan, WANG Zhen-fu, QIN Li and NING Yong-qiang, *Optoelectronics Letters* **6**, 421 (2010).
- [3] Jianjun Gao, *Journal of Lightwave Technology* **28**, 1332 (2010).
- [4] G. Verschaffelt, G. Craggs, M. L. F. Peeters, S. K. Mandre, H. Thienpont and I. Fischer, *IEEE Journal of Quantum Electronics* **45**, 249 (2009).
- [5] P. O. Leisher, A. J. Danner, J. J. Raftery Jr, D. Siriani and K. D. Choquette, *IEEE Journal of Quantum Electronics* **42**, 1091 (2006).
- [6] R. Safaisini, J. R. Joseph and K. L. Lear, *IEEE Journal of Quantum Electronics* **46**, 1590 (2010).
- [7] SHI Jing-jing, TIAN Zhen-hua, QIN Li, ZHANG Yan, WANG Zhen-fu, LIANG Xue-mei, YANG Ye, NING Yong-qiang, LIU Yun and WANG Li-jun, *Journal of Optoelectronics • Laser* **21**, 1446 (2010). (in Chinese)
- [8] P. Debernardi, *IEEE Journal of Quantum Electronics* **45**, 979 (2009).
- [9] A. A. Dyomin, V. V. Lysak, S. I. Petrov, Y. T. Lee and I. A. Sukhoivanov, *Optics and Lasers in Engineering* **46**, 211 (2008).
- [10] L. Piskorski, R. P. Sarza and W. Nakwaski, *Microelectronics Journal* **39**, 638 (2008).
- [11] H. Zhang, G. Mrozynski, A. Wallrabenstein and J. Schrage, *IEEE Journal of Quantum Electronics* **40**, 18 (2004).
- [12] Z. D. Kaftroudi and E. Rajaei, *Optics Communications* **284**, 330 (2011).
- [13] ZHAO Hong-dong, SONG Dian-you, ZHANG Zhi-feng, SUN Jing, SUN Mei, WU Yi and WEN Xing-rao, *Acta Physics Sinica* **53**, 3744 (2004). (in Chinese)